Analysis of the Vibronic Structure in the Emission and Absorption Spectra of (μ-1,1-Dicyanoethylene-2,2-dithiolato-*S*,*S*′)bis(triphenylphosphine)digold(I) and Assignment of the Emissive State

Stephen D. Hanna and Jeffrey I. Zink*

Department of Chemistry and Biochemistry, University of California, Los Angeles, California 90095

Received February 24, 1995[⊗]

Both the 77 K single crystal absorption and 20 K emission spectrum of (μ-1,1-dicyanoethylene-2,2-dithiolato-*S*,*S*′)bis(triphenylphosphine)digold(I), $(AuPPh_3)_2$[i-MNT], show resolved vibronic structure. Progressions in the 1410 cm^{-1} C═C stretching mode of the dithiolate ligand, and in the 480 cm^{-1} mode, which involves gold−dithiolate stretching, are observed in the emission spectrum. The resonance Raman spectra of the title compound and related compounds were used to identify the modes that give rise to the vibronic structure observed in the emission spectrum. The emission spectrum is fit using the time dependent theory of electronic spectroscopy. The theoretical fit to the spectrum requires distortions in vibrations involving both the metal−sulfur and dithiolate centered modes. These distortions show that the transition is a charge transfer involving the gold and the dithiolate ligand. The emission spectrum of an analogous complex, $(AuAsPh_3)_2$[i-MNT], is red shifted relative to the title complex. This red shift allows the direction of the charge transfer emission in the title complex to be assigned as a dithiolate to gold, ligand to metal charge transfer.

Introduction

In 1989 King et al. reported the luminescence of the title compound and several related complexes.[1] They noted that many of these dinuclear gold(I) compounds have large Stokes shifts which indicate large geometric changes in their excited states. Other researchers have also reported a variety of luminescent dinuclear gold(I) complexes.[2−4] The emission of several dinuclear bis(phosphine) complexes was assigned to metal centered transitions.[1,2d,5] In several gold phosphine thiolate complexes (mono- and dinuclear), however, the emission was assigned to a sulfur π to gold 6p ligand to metal charge transfer.[6,7] Many mononuclear gold complexes are also luminescent.[8−10]

Previous studies in our laboratory have focused on using vibronic structure that is observed in the emission spectra of a variety of compounds to assist in both the assignment of the excited states and the determination of the excited state geometries. In the tetranuclear Cu(I) cluster, Cu_4I_4(1-phenyl-3,4-dimethylphosphole)$_4$, vibronic structure was used to assign the luminescence to a metal to phosphole charge transfer.[11] Similar studies on the emission spectrum of (hexafluoroacetylacetonato)dimethylgold(III) and the absorption spectrum of (1,2-dicyanoethylene-1,2-dithiolato-*S*,*S*′)(biacetyl bisaniline)-nickel(II) used vibronic structure to assign the bands to intraligand charge transfer and ligand to ligand charge transfer, respectively.[12,13]

Single crystal absorption spectroscopy of (μ-1,1-dicyanoethylene-2,2-dithiolato-*S*,*S*′)bis(triphenylphosphine)digold(I), $(AuPPh_3)_2$[i-MNT], at 77 K reveals a forbidden transition with well-resolved vibronic structure. The 20 K emission spectrum also displays vibronic structure which is well enough resolved to allow a detailed analysis to be made and the bond length distortions to be calculated. This information aids in the assignment of the emissive state.

In this paper the vibronic structure that occurs in the low-temperature emission and single-crystal absorption spectra of the title compound is reported and analyzed. The information contained in these spectra is combined with data from the resonance Raman spectrum to help provide a more detailed description of the lowest energy excited state of the molecule. By comparing the spectral properties of $[n\text{-}Bu_4N]_2[Au_2(i\text{-}MNT)_2]$ and $(AuAsPh_3)_2$[i-MNT] with the title compound, a definitive assignment of the emissive state is made.

Experimental Section

I. Reagents. Sodium tetrachloroaurate(III) dihydrate (Aldrich), silver nitrate (Mallinckrodt), carbon disulfide (Mallinckrodt), potassium methoxide (Aldrich), triphenylarsine (Pfaltz and Bauer), and chloro(triphenylphosphine)gold(I) (Strem) were used as received. Methanol (Aldrich) was distilled over calcium hydride. Methylene chloride (Fisher) was distilled over phosphorus pentoxide. Malononitrile

[⊗] Abstract published in *Advance ACS Abstracts,* December 1, 1995.

(1) King, C.; Wang, J. C.; Khan, M. N. I.; Fackler, J. P., Jr. *Inorg. Chem.* **1989**, 28, 2145.
(2) (a) Che, C. M.; Wong, W. T.; Lai, T. F.; Kwong, H. L. *J. Chem. Soc., Chem. Commun.* **1989**, 243. (b) Che, C. M.; Kwong, H. L.; Yam, V. W. W.; Cho, K. C. *J. Chem. Soc., Chem. Commun.* **1989**, 885. (c) Yam, V. W. W.; Lai, T. F.; Che, C. M. *J. Chem. Soc., Dalton Trans.* **1990**, 3747. (d) Che, C. M.; Kwong, H. L.; Poon, C. K.; Yam, V. W. W. *J. Chem. Soc., Dalton Trans.* **1990**, 3215.
(3) (a) Schaefer, W. P.; Marsh, R. E.; McCleskey, T. M.; Gray, H. B. *Acta Crystallogr., Sect. C.* **1991**, *C47*, 2553. (b) McCleskey, T. M.; Gray, H. B. *Inorg. Chem.* **1992**, *31*, 1733.
(4) Lin, I. J. B.; Liu, C. W.; Liu, L. K.; Wen, Y. S. *Organometallics* **1992**, *11*, 1447.
(5) Jaw, H. R. C.; Savas, M. M.; Rogers, R. D.; Mason, W. R. *Inorg. Chem.* **1989**, 28, 1028.
(6) (a) Narayanaswamy, R.; Young, M. A.; Parkhurst, E.; Ouellette, M.; Kerr, M. E.; Ho, D. M.; Elder, R. C.; Bruce, A. E.; Bruce, M. R. M. *Inorg. Chem.* **1993**, *32*, 2506. (b) Jones, W. B.; Yuan, J.; Narayanaswamy, R.; Young, M. A.; Elder, R. C.; Bruce, A. E.; Bruce, M. R. M. *Inorg. Chem.* **1995**, *34*, 1996.
(7) Brown, D. H.; McKinlay, G.; Smith, W. E. *J. Chem. Soc., Dalton Trans.* **1977**, 1874.
(8) King, C.; Khan, M. N. I.; Staples, R. J.; Fackler, J. P. *Inorg. Chem.* **1992**, *31*, 3236.
(9) Larson, L. J.; McCauley, E. M.; Weissbart, B.; Tinti, D. S. *J. Phys. Chem.* **1995**, *99*, 7218.
(10) (a) Chan, C. W.; Wong, W. T.; Che, C. M. *Inorg. Chem.* **1994**, *33*, 1266. (b) Cheung, T. C.; Lai, T. F.; Che, C. M. *Polyhedron* **1994**, *13*, 2073.
(11) Lai, D. C.; Zink, J. I. *Inorg. Chem.* **1993**, *32*, 2594.
(12) Wexler, D.; Zink, J. I. *J. Phys. Chem.* **1993**, *97*, 4903.
(13) Wootton, J. L.; Zink, J. I. *J. Phys. Chem.* **1995**, *99*, 7251.

0020-1669/96/1335-0297$12.00/0

(Kodak) was distilled under vacuum prior to use. Absolute ethanol (Quantum), acetone (Fisher), chloroform (Fisher), and anhydrous ethyl ether (Fisher) were used as received.

II. Synthesis. Potassium 1,1-dicyanoethylene-2,2-dithiolate, K_2[i-MNT], and $(AuPPh_3)_2$[i-MNT] were synthesized by the literature method.[14,15] The latter compound was recrystallized by slow diffusion of diethyl ether into a methylene chloride solution of $(AuPPh_3)_2$[i-MNT]. Synthesis was confirmed by X-ray powder diffraction.[15]

$[n\text{-}Bu_4N]_2[Au_2(i\text{-}MNT)_2]$ was synthesized according to the published procedure.[16,17] The compound was recrystallized by slow diffusion of diethyl ether into a methylene chloride solution of $[n\text{-}Bu_4N]_2[Au_2(i\text{-}MNT)_2]$. Synthesis was confirmed by Raman spectroscopy (ν(C≡N) = 2200 cm^{-1}) and by emission spectroscopy.[1,16,17]

Chloro(triphenylarsine)gold(I) was synthesized in an analogous fashion to the synthesis of chloro(triphenylphosphine)gold(I).[18] Sodium tetrachloroaurate(III) dihydrate (0.25 g, 0.625 mmol) was dissolved in a 1:1 solution of ethanol and acetone (10 mL). Triphenylarsine (0.383 g, 1.25 mmol) was dissolved in chloroform (2 mL) and added to the gold salt solution. Upon addition the solution became cloudy. The solution was stirred uncovered for 1 h and then cooled for 1 h in a 4 °C refrigerator to induce precipitation of the product. The product, a white powder, was collected by vacuum filtration and rinsed with cold ethanol; yield, 90%.

$(AuAsPh_3)_2$[i-MNT] was synthesized in a similar fashion to the synthesis of $(AuPPh_3)_2$[i-MNT],[15] except $ClAuAsPh_3$ was used instead of $ClAuPPh_3$. $ClAuAsPh_3$ (0.10 g, 0.184 mmol) was dissolved in methylene chloride (60 mL). K_2[i-MNT] (0.020 g, 0.093 mmol) was dissolved in methanol (15 mL) and added dropwise (1 drop/(10 s)) to the $ClAuAsPh_3$ solution. The resulting solution was stirred overnight and then filtered over celite to yield a pale yellow solution. The solvent was removed by evaporation in a vacuum to give 0.085 g of the yellow powder; yield, 80%. The compound decomposes in air over a period of months. Anal. Calcd for $Au_2C_{40}H_{30}As_2S_2N_2$: C, 41.90; H, 2.64; N, 2.44; Au, 34.36. Found: C, 39.21; H, 2.8; N, 2.21; Au, 35.88. IR (KBr pellet, cm^{-1}): ν(C≡N), 2201 (sharp); ν(C═C), 1631 (broad, phenyl).

Elemental analysis was performed by Galbraith Laboratories Inc.

III. Spectroscopic Measurements. Luminescence spectra at 20 K were taken using a Spex 1702 single monochromator equipped with a Stanford Research Systems SR400 photon counter and an RCA C31034 photomultiplier tube or a Hamamatsu R316−02 red sensitive photomultiplier tube. The 351 nm line of an argon ion laser was typically used for excitation, although spectra were also measured using the 363 and 413 nm lines from a krypton ion laser or the 457 nm line from an argon ion laser. Data were collected on an IBM PC computer. Solid samples were cooled inside an Air Products displex closed-cycle helium refrigerator equipped with a thermocouple. Peak locations are accurate to ±20 cm^{-1}. All data were corrected for instrumental response.

Infrared Spectra were obtained from KBr pellets on a Nicolet Instruments Model 510P FT-IR spectrometer. Peak locations are accurate to ±5 cm^{-1}.

Raman spectra were taken using a Jobin-Yvon 320/640 triple monochromator equipped with a 256 × 1024 Princeton Instruments liquid nitrogen cooled CCD. Data were collected using an IBM PC computer. Excitation was provided by either a Coherent I90-6 argon ion laser, or a Coherent I90-K krypton ion laser. The excitation wavelengths used were 413.1, 457.9, 514.5 nm, and 647.1 nm. Raman samples were prepared by diluting the compound in powdered KBr to prevent thermal decomposition. Scattered light was collected at 90° relative to the laser beam. Peak locations are accurate to ±5 cm^{-1}.

Solution absorption spectra were obtained from methylene chloride solutions using a Shimadzu UV260 absorption spectrometer. Quartz cuvettes having a 1 cm path length were used. Typical concentrations were on the order of 10^{-5} M.

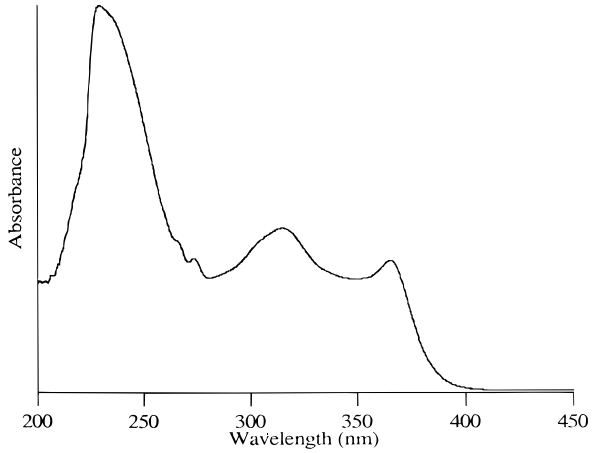

Figure 1. Solution absorption spectrum of $(AuPPh_3)_2$[i-MNT] in methylene chloride.

Single-crystal polarized absorption spectra were obtained using an instrument described previously.[19,20] The crystal used was grown by slow diffusion of ethyl ether into a methylene chloride solution of $(AuPPh_3)_2$[i-MNT]. The absorption spectrum was measured with light polarized along an extinction axis of the crystal and at 90° relative to this axis.

Emission lifetimes were measured at 20 K using 406 nm excitation from an excimer pumped dye laser. Data were collected using a Spex 1702 single monochromator equipped with an RCA C31034 photomultiplier tube and a Tektronix RTD-710 transient digitizer. The time constant of the instrument was an order of magnitude smaller than the luminescence lifetime.

Results

I. Spectroscopic Studies of $(AuPPh_3)_2$[i-MNT]. (a) Absorption. Figure 1 shows the solution absorption spectrum of $(AuPPh_3)_2$[i-MNT] measured in methylene chloride. The spectrum shows several features below 350 nm. The lowest apparent absorption maximum is at 365 nm, having an extinction coefficient of 14 000 M^{-1} cm^{-1}. Close inspection reveals a weak shoulder ($\epsilon \approx 10$ M^{-1} cm^{-1}) at 400 nm. This shoulder was studied more closely using single-crystal absorption spectroscopy.

Thick crystals of $(AuPPh_3)_2$[i-MNT] were grown in order to examine the lowest energy absorption. The single-crystal absorption spectrum shown in Figure 2 (left) reveals the presence of resolved vibronic structure in the region where the low-energy shoulder was observed in the solution spectrum. The peak maxima are listed in Table 1. The spectrum consists of three groupings, each containing three peaks. The average spacings between each group is 1270 cm^{-1}. The spacing between members of the groups is on average 440 cm^{-1}. Both spacings decrease toward the high-energy side of the spectrum. When the spectrum is taken using the orthogonal extinction direction, the total intensity of the spectrum decreases, but the relative intensities of all absorbances to each other remain unchanged.

(b) Emission. The low-temperature emission spectrum of $(AuPPh_3)_2$[i-MNT] has vibronic features similar to those observed in the single-crystal absorption (see Figure 2 (right)). The spectrum is broad with a full width at half-maximum amplitude (fwhm) of 2000 cm^{-1} and is asymmetric. The peak maximum occurs at 21 655 cm^{-1}. The lifetime of this luminescence is approximately 2 μs and is not exponential. The emission spectrum shows well-resolved vibronic structure with

(14) Gompper, R.; Topfl, W. *Chem Ber.* **1962**, *95*, 2871.
(15) Khan, M. N. I.; Wang, S.; Heinrich, D. D.; Fackler, J. P., Jr. *Acta Crystallogr., Sect. C.* **1988**, *C44*, 822.
(16) Khan, M. N. I.; Wang, S.; Fackler, J. P., Jr. *Inorg. Chem.* **1989**, *28*, 3579.
(17) Khan, M. N. I.; Fackler, J. P., Jr.; King, C.; Wang, J. C.; Wang, S. *Inorg. Chem.* **1988**, *27*, 1672.
(18) McAuliffe, C. A.; Parish, R. V.; Randall, D. P. *J. Chem. Soc., Dalton Trans.* **1979**, 1730.
(19) Chang, T. H.; Zink, J. I. *J. Am. Chem. Soc.* **1986**, *108*, 5830.
(20) Reber, C.; Zink, J. I. *Inorg. Chem.* **1991**, *30*, 2994.

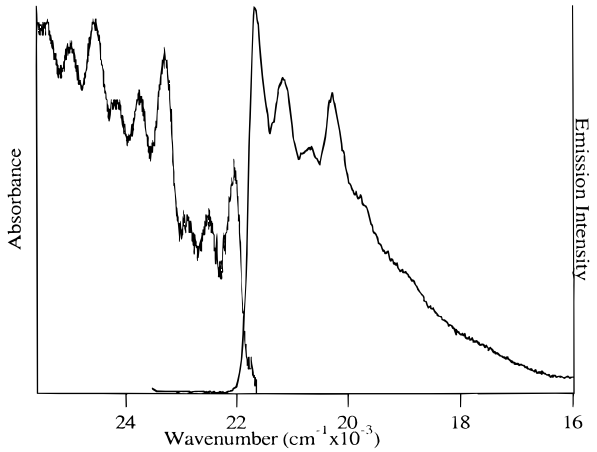

Figure 2. Crystal absorption spectrum (left) and 20 K emission spectrum (right) of $(AuPPh_3)_2$[i-MNT].

Table 1. Position of Band Maxima in the Low-Temperature Single-Crystal Absorption Spectrum of $(AuPPh_3)_2$[i-MNT]

mode	freq (cm^{-1})	mode	freq (cm^{-1})
ϵ_{00}	22 017	$\epsilon_{00} + \nu_{1410} + 2\nu_{480}$	24 166
$\epsilon_{00} + \nu_{480}$	22 487	$\epsilon_{00} + 2\nu_{1410}$	24 552
$\epsilon_{00} + 2\nu_{480}$	22 894	$\epsilon_{00} + 2\nu_{1410} + \nu_{480}$	24 988
$\epsilon_{00} + \nu_{1410}$	23 288	$\epsilon_{00} + 2\nu_{1410} + 2\nu_{480}$	25 445
$\epsilon_{00} + \nu_{1410} + \nu_{480}$	23 753		

Table 2. Position of Band Maxima in the Emission Spectrum of $(AuPPh_3)_2$[i-MNT]

mode	freq (cm^{-1})	mode	freq (cm^{-1})
ϵ_{00}	21 655	$\epsilon_{00} + \nu_{1410}$	20 263
$\epsilon_{00} + \nu_{480}$	21 164	$\epsilon_{00} + \nu_{1410} + \nu_{480}$	19 782
$\epsilon_{00} + 2\nu_{480}$	20 683		

a progression having a spacing of 1410 cm^{-1} and a second progression having a spacing of 480 cm^{-1}. The peak maxima are listed in Table 2. The pattern of the spacings is similar to that observed in the absorption spectrum, however, these spacings are larger than those in the absorption spectrum by about 10%. The spectrum of this molecule is insensitive to changes in excitation wavelength. Spectra taken using 351, 363, 413, and 457 nm excitation are virtually identical.

Emission spectra of $(AuPPh_3)_2$[i-MNT] often show a low-energy shoulder due to the emission from unreacted K_2[i-MNT]. This shoulder can be eliminated by repeated recrystallizations.

(c) Raman. Raman spectroscopy was used as an aid for assigning the vibronic structure present in the emission and absorption spectrum of $(AuPPh_3)_2$[i-MNT]. Figure 3 shows the Raman spectrum of $(AuPPh_3)_2$[i-MNT] from 200 to 1500 cm^{-1}. The best spectra were obtained using the 413.1 nm line from a Kr ion laser. This line is in preresonance with the absorption at 365 nm but is in resonance with the lowest excited state that gives rise to the structured absorption band. Table 3 lists the most intense bands observed in the Raman spectrum. The compound is thermally unstable, and low laser powers must be used to prevent sample degradation. Sample degradation can also be prevented by taking spectra on samples diluted with powdered potassium bromide.

II. Spectroscopic Studies of Related Compounds. In the discussion of the assignments of the vibrational and electronic spectra, it will be necessary to have information on related compounds. Data relevant to the discussion of the spectroscopy of $(AuPPh_3)_2$[i-MNT] are presented below. The vibrational data of all compounds are summarized in Table 4.

(a) $(AuAsPh_3)_2$[i-MNT]. This molecule was studied because it is identical to the title compound except that a triphenylarsine

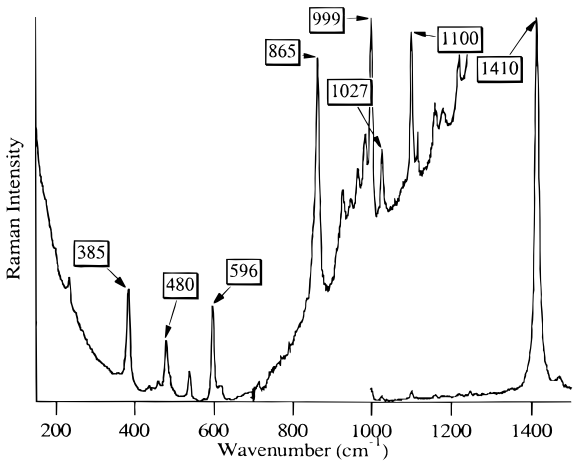

Figure 3. Resonance Raman spectrum of $(AuPPh_3)_2$[i-MNT] measured using the 413.1 nm line of a krypton ion laser.

Table 3. Raman Frequencies of $(AuPPh_3)_2$[i-MNT] and Assignments[a]

freq (cm^{-1})	assignmt	calcd displacement
385	ν(Au—P)	0.30
480	ν(Au—S)	1.26
596		0.10
865	ν(C—S)	0.65
999	phenyl p-ring	0.65
1027	b β(C—H)	0.10
1100	phenyl q x-sensitive	0.10
1410	ν(C═C)	1.05
2209	ν(C≡N)	0.20

[a] The displacements used in the best fit of the emission spectrum are also shown.

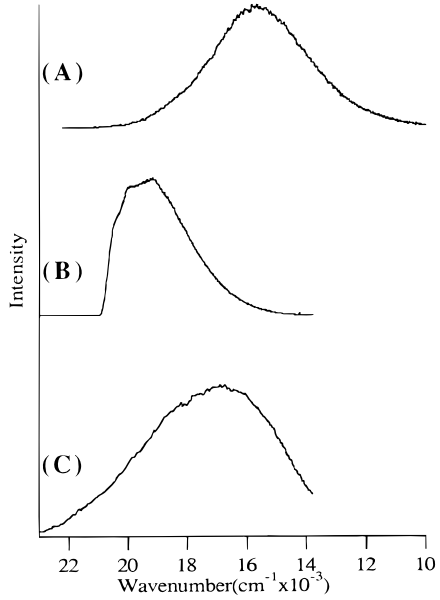

Figure 4. Emission spectrum of comparison compounds at 20 K: (a) $(AuAsPh_3)_2$[i-MNT]; (b) $[n\text{-}Bu_4N]_2[Au_2(i\text{-}MNT)_2]$; (c) K_2[i-MNT].

replaces a triphenylphosphine. This change allows us to observe the spectroscopic effects associated with replacing the phosphine group.

The low-temperature emission spectrum of $(AuAsPh_3)_2$[i-MNT] is shown in Figure 4 (top). This molecule is brightly luminescent at 20 K. While the onset of the emission of $(AuAsPh_3)_2$[i-MNT] is red shifted by 1500 cm^{-1} relative to the spectrum of $(AuPPh_3)_2$[i-MNT], the peak maximum is shifted by 6000 cm^{-1}. The emission maximum occurs at 15 650 cm^{-1} in this compound. This spectrum is also broader than the

Table 4. Vibrational Frequencies and Assignments for $(AuPPh_3)_2$[i-MNT] and Comparison Compounds[a]

	freq								
compd	ν(Au−S)	ν(C−S)	p-ring	ν(Au−P)	ν(C≡N)	ν(C=C)	ν(Au−Cl)	b β(C−H)	q x-sensitive
K_2[i-MNT]$_2$	−	870 (IR)	−	−	2177 (IR)	1421	−	−	−
$(AuPPh_3)_2$[i-MNT]	480	865	999	385	2209	1410	−	1027	1100
[Au(i-MNT)]$_2$	479/492	856	−	−	2200	1376	−	−	−
$(AuAsPh_3)_2$[i-MNT]	467 (IR)		999 (IR)		2201 (IR)	1400 (IR)		1022 (IR)	1080 (IR)
$ClAuPPh_3$	−	−	998	−	−	−	327	1025	1101
$ClAuAsPh_3$	−	−	997	356	−	−	327	1023	1084

[a] Unless otherwise noted all data are from the Raman spectrum. [b] Incomplete data set, see text.

spectrum of $(AuPPh_3)_2$[i-MNT] with a fwhm = 3700 cm^{-1}. This spectrum shows no sign of vibronic structure.

The infrared spectrum of $(AuAsPh_3)_2$[i-MNT] contains bands at 2201, 1400, 1080, 1022, 999, and 467 cm^{-1} that are at frequencies similar to those observed in the title compound. Raman data on this compound are unavailable because the molecule is a poor Raman scatterer. Efforts to obtain a spectrum by using higher laser powers only resulted in the decomposition of the sample.

(b) $[n\text{-}Bu_4N]_2[Au_2(i\text{-}MNT)_2]$. This compound was studied because it contains only the dithiolate ligand and no phosphine ligands. This compound allows us the opportunity to isolate the spectroscopic features that are due to the gold−dithiolate moiety.

The 77 K emission spectrum of this compound has been reported previously.[1] The 20 K emission spectrum is shown in Figure 4 (middle). The onset of the emission of $[n\text{-}Bu_4N]_2[Au_2(i\text{-}MNT)_2]$ is shifted by 1250 cm^{-1} relative to $(AuPPh_3)_2$[i-MNT]. The spectrum has a fwhm = 2800 cm^{-1}.

The Raman spectrum of this compound shows the expected normal modes due to the [i-MNT] ligands. Vibrational modes are observed at 2200, 1376, 856, and 479 cm^{-1}.

(c) $ClAuPPh_3$. The luminescence of this molecule has been reported previously.[1] The luminescence maximum occurs at approximately 20 400 cm^{-1}. Relevant vibrational modes are observed at 1101, 1025, 998, and 327 cm^{-1} in the Raman spectrum.

(d) $ClAuAsPh_3$. This Raman spectrum of this compound was studied to identify modes that might be present in related compounds. As with the phosphine complexes, this complex has several modes due to the phenyl groups attached to the arsine. Raman bands are observed at 327, 356, 998, 1022, and 1084 cm^{-1}.

(e) K_2[i-MNT]. This compound was studied to determine if the uncoordinated ligand is luminescent and to aid in the assignment of vibrational modes due to the dithiolate ligand. The 20 K emission spectrum of K_2[i-MNT] is shown in Figure 4 (bottom). The luminescence spectrum is broad and featureless, having fwhm = of 5400 cm^{-1}. The peak maximum occurs at 16 800 cm^{-1}.

Vibrational bands relevant to this discussion were studied by IR and Raman spectroscopy. Vibrational modes at 2177 and at 870 cm^{-1} are observed in the IR spectrum. Raman spectra of this compound are difficult to measure as the compound is a very poor Raman scatterer. Using higher laser powers results in decomposition of the sample. Previous surface enhanced Raman experiments have shown the presence of the C≡N stretch between 2196 and 2206 cm^{-1} and of the C=C stretch between 1380 and 1423 cm^{-1}, depending on applied electric potential.[21] In our Raman spectrum the only discernible band above the large background is a mode at 1421 cm^{-1}.

(21) Takahashi, M.; Kano, Y.; Inukai, J.; Ito, M. *Chem. Phys. Lett.* **1992**, *196*, 70.

Discussion

I. Assignment of Raman Peaks. The assignment of the normal modes of $(AuPPh_3)_2$[i-MNT] is assisted by comparing the Raman spectra of the various compounds studied. The presence or absence of a mode in a series of compounds can be correlated with the presence or absence of a given ligand. This information can then be used to assign the mode as a dithiolate centered mode or as a phosphine centered mode. After the assignments of the vibrational modes are established, the vibronic structure observed in the electronic spectra of $(AuPPh_3)_2$-[i-MNT] can be interpreted.

In the parent compound a peak is observed in the Raman spectrum at 2209 cm^{-1}. This peak is due to the ν(C≡N). This assignment is confirmed by both literature precedent and the fact that in our study the only compounds having Raman bands in this region are those containing the [i-MNT]$^{2-}$ ligand (see Table 3).[21] The peak at 1410 cm^{-1} is assigned to the ν(C=C) of the dithiolate ligand. This is the same assignment that was given previously in the bare ligand.[21] This peak is absent in the Raman spectrum of $ClAuPPh_3$.

The ν(Au−P) in the title compound is observed at 385 cm^{-1}. This value is typical for gold−phosphorus stretching frequencies.[18] No peaks are observed in this location for compounds that do not contain a Au−P linkage. The ν(Au−As) for $ClAuAsPh_3$ is observed at 356 cm^{-1}. The Au−Cl stretch is observed at 327 cm^{-1} in both $ClAuPPh_3$ and $ClAuAsPh_3$.[18]

The peak observed at 480 cm^{-1} in $(AuPPh_3)_2$[i-MNT] is assigned to a group mode involving significant Au−S stretching. This assignment is supported by the normal coordinate analysis of this compound.[22] This mode is observed in the three compounds having two gold centers bound to the dithiolate ligand. This vibration is not observed in the Raman spectra of the simple mononuclear gold−phosphine complexes or in that of the bare ligand.

There is a peak in the Raman spectrum of the parent compound at 865 cm^{-1}. A similar peak is observed in the Raman spectra of $[n\text{-}Bu_4N]_2[Au_2(i\text{-}MNT)_2]$. The ν(C−S) for the related (1,2-dicyanoethylene-1,2-dithiolato)(ethylene)nickel-(II) complex is observed at 866 cm^{-1}.[23,24] On the basis of this comparison, the 865 cm^{-1} mode is assigned as the carbon−sulfur stretching frequency of the [i-MNT]$^{2-}$ ligand.

The final modes that are important to this discussion are the three peaks observed at 999, 1027, and 1100 cm^{-1} in the Raman spectra of all of the compounds containing phenyl groups. These modes have previously been assigned as being associated with phenyl ring modes.[25] The band at approximately 999 cm^{-1} has previously been assigned as a phenyl p-ring mode.[25] The peak observed at 1027 cm^{-1} is assigned as the b β(C−H) of the phenyl rings, and the peak at 1100 cm^{-1} is assigned to the q x-sensitive phenyl ring mode.[25]

(22) Diaz-Flemming, G. Private communication.
(23) Clark, R. J. H.; Turtle, P. C. *J. Chem. Soc., Dalton Trans.* **1977**, 2142.
(24) Schläpfer, C. W.; Nakamoto, K. *Inorg. Chem.* **1975**, *14*, 1338.
(25) Wiffen, D. H. *J. Chem. Soc.* **1956**, 1350.

II. Relationship between the Emission and Absorption Spectra of $(AuPPh_3)_2$[i-MNT]. The single-crystal absorption spectrum and the luminescence spectrum of $(AuPPh_3)_2$[i-MNT] both contain resolved vibronic structure (see Figure 2). On first glance the two spectra appear fairly similar. Both spectra have resolved progressions in two modes (one having a frequency about 3 times the magnitude of the other). On the basis of the Raman studies discussed in the previous section, the high frequency mode is assigned as the carbon−carbon double bond stretch of the dithiolate ligand, and the low-frequency mode is assigned as being due to a group mode having a large contribution from the gold−sulfur stretch (see Table 3).

On closer inspection, however, several key differences become apparent. The vibrational spacings in the emission spectrum are 480 and 1410 cm^{-1}, while in the absorption spectrum the corresponding spacings decrease by approximately 10% to 441 and 1268 cm^{-1}, respectively. Thus, there is a decrease in the force constant of these two modes in the excited state of the molecule. In the emission spectrum, the intensity maximum occurs in the first quanta. This result indicates that there are relatively small distortions in the excited state of this molecule along these normal coordinates. Unlike the emission spectrum, the spacing in the absorption spectrum gets smaller toward the high-energy end of the spectrum. This indicates that, in addition to the change in the force constant in the excited state, the excited state potential energy surface is anharmonic.

The vibronic structure observed in the single-crystal absorption spectrum is also better resolved than that of the emission spectrum. In the absorption spectrum the structure is well enough resolved that three replicates of three peaks are observed, while in the emission spectrum by the second peak of the second replicate the structure is largely washed out.

III. Calculation of Excited State Distortions. The emission spectrum is modeled theoretically using the time dependent theory of electronic spectroscopy.[26−28] In the time dependent picture, when a photon is emitted, a wavepacket, ϕ, is produced on the ground state surface. Since this wavepacket results from a vertical transition from the excited state, it is not an eigenfunction of the ground state. The nonstationary wavepacket will then evolve in time obeying the time dependent Shrödinger equation. The emission spectrum is determined by the dynamics of the wavepacket on the ground state potential energy surface.[29] The emission spectrum is given by

$$I(\omega) = C\omega^{e}\int_{-\infty}^{+\infty}\exp(i\omega t)\langle\phi|\phi(t)\rangle\,dt \qquad (1)$$

where $I(\omega)$ is the emission intensity in photons per unit volume per unit time at the frequency ω and C is a constant. The most important part of eq 1 is $\langle\phi|\phi(t)\rangle$, which is the autocorrelation function of the initial wavepacket, ϕ, and the wavepacket as it evolves in time, $\phi(t)$. The initial wavepacket $\phi(t = 0)$ is the lowest energy eigenfunction of the excited state potential energy surface multiplied by the transition dipole moment. Methods for calculating the autocorrelation function have been discussed in the literature.[26−29]

The autocorrelation function depends strongly on the displacement, Δ, of the ground state potential energy surface along a normal coordinate relative to the minimum of the excited state potential energy surface. Changes in the values of the displacement along a normal coordinate will alter the intensity distribution in a calculated spectrum. Larger displacements result in a progression achieving its maximum intensity at later quanta, while small distortions shift the intensity toward earlier quanta.

In general displacements occur along several of the normal coordinates of the molecule. In the case where there are multiple uncoupled normal modes the total overlap is given by

$$\langle\phi|\phi(t)\rangle = \prod_k\langle\phi_k|\phi_k(t)\rangle\exp(-iE_0t - \Gamma^2t^2) \qquad (2)$$

where E_0 is the difference in the electronic energy between the minimum of the two surfaces and Γ is a damping factor.

The values of the displacement of the normal coordinate, Δ, are unitless and do not provide information about the sign. They can be converted into individual bond length distortions that occur in the excited state of the molecule by employing the following equation:

$$\delta = \left[\frac{6.023\times10^{23}}{m}\frac{\hbar}{2\pi c\omega}(10^8)\Delta\right]^{1/2} \qquad (3)$$

where δ is the distortion of the mode in angstroms, m is the mass involved in the vibration in units of gram atomic weight, and Δ is the dimensionless displacement of the ground state potential energy surface.

The only adjustable parameters used in these calculations are the unitless displacements, Δ , and the damping factor, Γ, which affects the breadth of the peaks. While the anharmonicity of the potential surfaces and the changes in force constants between the ground and excited state could be treated with this theory, inclusion of these factors causes only small changes in the calculated values of Δ and are not treated here. This theoretical treatment is similar to a Franck−Condon analysis. For a more detailed discussion of the theory the reader is referred to the literature.[29]

In order to fit the emission spectrum of $(AuPPh_3)_2$[i-MNT] at least two modes, the 480 and the 1410 cm^{-1} modes, must be used, because they are observed directly in the vibronic structure of the spectrum. The value of E_0, 21 655 cm^{-1}, used in these calculations is also taken directly from the experimental spectrum. If, however, only the above two modes are used, a satisfactory fit cannot be obtained. The best fit is obtained with $\Delta(480\ cm^{-1}) = 1.28$, and $\Delta(1410\ cm^{-1}) = 1.03$. The fit to the first two peaks is in excellent agreement with the experimental spectrum. However, the two mode model fails to fit the third feature of the experimental spectrum and the intensity of the second group of peaks.

The major inconsistency between the spectrum calculated using only two modes and the experimental spectrum is a dip in the calculated spectrum that occurs at approximately 950 cm^{-1} from the E_0. In the Raman spectrum of $(AuPPh_3)_2$[i-MNT] two intense bands are observed at a frequency near 950 cm^{-1}. By including the observed vibrations at 999 and 865 cm^{-1}, a good fit to the experimental spectrum can be obtained. In this fit the distortions of the 1410 and 480 cm^{-1} modes and the value of Γ are almost unchanged from those calculated in the two mode fit discussed above. The distortions for both of the other modes are 0.65.

To minimize bias in the fitting of the experimental spectrum, a final fit using all of the most intense modes in the Raman spectrum that are at least as intense as the 480 cm^{-1} mode was calculated. The intensity of a resonance Raman peak is related to the magnitude of the distortion of the normal mode giving rise to that peak.[27,29] (Qualitatively, the most intense peaks correspond to the modes with the largest distortions. Quantitative values cannot be simply obtained for $(AuPPh_3)_2$[i-MNT]

(26) Heller, E. J. *J. Chem. Phys.* **1978**, *68*, 2066.
(27) Tannor, D. J.; Heller, E. J. *J. Chem. Phys.* **1982**, *77*, 202.
(28) Heller, E. J. *Acc. Chem. Res.* **1981**, *14*, 368.
(29) Zink, J. I.; Shin, K. S. *Advances in Photochemistry*; Wiley: New York, 1991; Vol. 16, p 119.

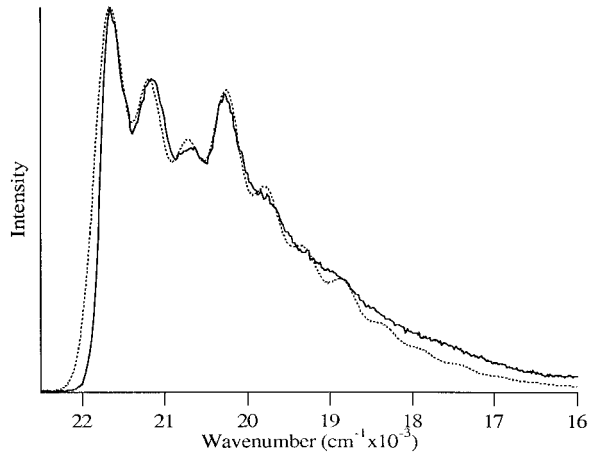

Figure 5. Calculated emission spectrum of $(AuPPh_3)_2$[i-MNT] (dotted line) compared to the experimental spectrum (solid line).

because of the overlap of the absorption bands.) The best calculated spectrum is compared to the experimental spectrum in Figure 5. The distortions used in the fit are shown in Table 3. As in all of the fits discussed, a damping factor of 125 cm^{-1} was used. The best fit obtained matches the experimental data well; peak locations and intensities are well-matched.

The values of Δ calculated for the two most important modes are almost unchanged from those used in the two mode fit; Δ(480 cm^{-1}) changes from 1.28 to 1.26 , and Δ(1410 cm^{-1}) changes from 1.03 to 1.05. Inclusion of the additional modes "fill in" the spectrum without dramatically changing these displacements. The fit is very sensitive to the magnitude of the displacement for the two modes that appear most prominently in the experimental spectrum, and the value of these Δs can be more accurately determined than those of modes which merely serve to fill in the spectrum.

The unitless displacements used to fit the experimental spectrum are directly related to the bond length changes in the excited state of the molecule. A rigorous calculation of these changes requires a full normal coordinate analysis. An estimate of the bond length distortions can be obtained by making some simple assumptions about the reduced mass of the ligands. The two most distorted modes in the molecule are the 480 cm^{-1} mode and the 1410 cm^{-1} mode. By assuming that the 480 cm^{-1} mode is due only to an isolated Au−S stretch (a gross approximation), $\Delta = 1.26$ would correspond to a bond length change of 0.06 Å in the excited state. By assuming that the 1410 cm^{-1} mode is due to an isolated C═C stretch (a better approximation), $\Delta = 1.05$ would correspond to a bond length change of 0.07 Å in the excited state.

IV. Assignment of the Emitting State. On the basis of the spectroscopic data discussed above, an assignment for the emissive state of $(AuPPh_3)_2$[i-MNT] can be made. The calculated spectrum of $(AuPPh_3)_2$[i-MNT] requires significant distortions in the 480 cm^{-1} gold−dithiolate group mode and in the 1410 cm^{-1} carbon−carbon double bond stretch of the dithiolate ligand. The requirement of dithiolate centered modes and modes that involve the gold centers suggests that the electronic transition that gives rise to the luminescence in $(AuPPh_3)_2$[i-MNT] is a charge transfer between the gold centers and the $[i\text{-}MNT]^{2-}$ ligand. By changing the distribution of electron density around the gold centers and the $[i\text{-}MNT]^{2-}$ ligand, Au−S and the dithiolate C═C bond lengths will be changed. Interligand, and metal centered transitions would be expected to lead to distortions in different normal modes of the molecule.

The direction of the charge transfer transition (i.e., MLCT or LMCT) can be deduced by examining the luminescence of a related compound. The luminescence energy of the gold−dithiolate charge transfer is expected to shift as the energy of the metal orbitals is changed by varying the π and σ donor properties of the other ligands bound to the gold centers. Triphenylarsine is both a weaker π and σ donor than triphenylphosphine.[30] A weaker donor ligand will cause a smaller splitting of the gold 5d orbitals. Unoccupied orbitals on the dithiolate ligand are not expected to be dramatically affected by such a substitution. If the transition were a MLCT, the luminescence would be expected to shift to higher energy upon exchanging the triphenylphosphine group with a triphenylarsine group because the highest occupied molecular orbital (HOMO), a gold d orbital, is lowered in energy when the phosphine is replaced by an arsine. Because the luminescence of $(AuAsPh3)_2$-[i-MNT] shifts to lower energy (red shifts) relative to the parent compound, the emission is assigned as LMCT from the dithiolate to an unoccupied orbital primarily metal in character. This assignment is the same as that for related dinuclear and mononuclear gold complexes having both phosphine and thiolate ligands.[6,7] The low extinction coefficient of the lowest energy excited state in the single-crystal absorption spectrum indicates that the transition is weakly allowed. Theoretical[1] and spectroscopic studies[2d,5] of $[Au(Ph_2PCH_2PPh_2)]_2^{2+}$, $[Au(Me_2PCH_2PMe_2)]_2^{2+}$, and $[Au(H_2PCH_2PH_2)]_2^{2+}$ have suggested that this LUMO has substantial Au $6p_z$ orbital character directed along the gold−gold axis. Our experimental data for this compound do not allow us to identify the metal orbital.

Summary

In exploring the 77 K single-crystal absorption of $(AuPPh3)_2$-[i-MNT], a weak ($\approx$10 M^{-1} cm^{-1}) low-energy transition with well-resolved vibronic structure was discovered. The 20 K emission spectrum of this compound also displays vibronic structure which is well enough resolved for analysis. Progressions in both a 1410 cm^{-1} mode and a 480 cm^{-1} mode are observed in the emission.

The emission spectrum was fit using the time dependent theory of electronic spectroscopy in tandem with the vibrational frequencies and intensities measured in the resonance Raman spectrum. The most distorted normal coordinates of the molecule in the excited state are those which involve the gold−sulfur bonds and the $[i\text{-}MNT]^{2-}$ ligand. This result establishes the charge transfer nature of the electronic state that gives rise to the structured emission spectrum.

Comparison compounds were studied to establish the direction of the transition (i.e., MLCT or LMCT). The emission spectrum of an analogous complex, $(AuAsPh3)_2$-[i-MNT], was significantly red shifted relative to the phosphine complex. Because the triphenylarsine is a weaker field ligand, the red shift in the emission spectrum is consistent with the assignment of the transition as a ligand to metal charge transfer.

Acknowledgment. This work was made possible by a grant from the National Science Foundation (CHE 91-06471), and a Laboratory Graduate Fellowship from the Department of Defense and Air Force Office of Scientific Research (S.D.H.).

IC950210Q

(30) Chang, T. H.; Zink, J. I. *Inorg. Chem.* **1986**, *25*, 2736.